Local clothing properties for thermo-physiological modelling: comparison of methods and body positions

Authors: Miloš Fojtlín[1, 2], Agnes Psikuta[1*], Jan Fišer[2], Róbert Toma [2], Simon Annaheim[1], Miroslav Jícha[2]

[1]Empa Swiss Federal Laboratories for Material Science and Technology, Laboratory for Biomimetic Membranes and Textiles, St. Gallen, Switzerland

[2]Brno University of Technology, Faculty of mechanical engineering, Energy Institute, Department of Thermodynamics and Environmental Engineering, The Czech Republic

[*]Corresponding author: agnes.psikuta@empa.ch; Empa Swiss Federal Laboratories for Material Science and Technology, Lerchenfeldstrasse 5, 9014 St. Gallen, Switzerland

ABSTRACT

Thermo-physiological modelling has become a frequently used and valuable tool for simulations of thermoregulatory responses in a variety of applications, such as building and vehicular comfort studies. To achieve reliable results, it is necessary to provide precise inputs, such as clothing thermal parameters. These values are usually presented in a standing body position and scarcely reported locally for individual body parts. Moreover, as an air gap distribution is both highly affected by a given body position and critical for clothing insulation, this needs to be taken into account. Therefore, the aim of this study was to examine eight probable approaches to assess the clothing parameters using state-of-the-art measurements, analytical and empirical models, and estimation. Next, we studied the effects of the eight clothing inputs on predicted thermo-physiological response under the same environmental conditions conducted with the Fiala model. Secondly, the study focuses on differences between seated and standing positions, both using two clothing sets representing typical European, indoor, summer and winter ensembles. The results show clear differences in clothing thermal properties between sitting and standing positions on both lower limbs and torso. The outputs of the eight

examined methods showed discrepancies between them, in the range of up to 200%. The discrepancies from the eight clothing inputs were also propagated in the results of thermo-physiological responses. These varied significantly in terms of their impact on predicted thermal sensation, highlighting the importance of using adequate inputs for modelling.

KEYWORDS:

Clothing; **Thermal insulation; Evaporative resistance; Sitting; Clothing area factor; Thermal sensation;**

1 Introduction

Efforts to minimize energy expenditure for heating ventilation and air-conditioning (HVAC) in a variety of indoor environments – such as transportation and occupational settings – with help of local conditioning technologies are a subject to substantial research attention [1–4]. Effects of localised heating and cooling on a human thermo-physiological response are usually investigated in human or thermal manikin studies [5,6]. Alternatively, one can utilise validated thermo-physiological models that allow prompt simulations of human thermo-physiological responses and reduce the need for costly physical studies [7–9]. In addition, these responses can be further translated into the prediction of thermal sensation or thermal comfort using dedicated models [10].

At the same time, to accurately simulate thermal interactions between the human body and the surrounding environment, using thermo-physiological models, there is a need for precise inputs defining: the environmental conditions, metabolic activity, and clothing [11]. Clothing governs heat and mass transfer between the human body and the ambient environment. Local clothing thermal properties may vary considerably over the body, thus, having a major impact on the development of skin temperatures, sweating, and perception of thermal sensation and comfort [12]. Yet, these properties, namely intrinsic clothing insulation (I_{cl}), evaporative clothing resistance ($R_{e,cl}$), and clothing area factor (f_{cl}), are rarely reported in literature [11]. Moreover, previous research has shown that body posture change has a significant impact on the resulting global clothing properties [13–15], however, only globally as an average for the whole body. The findings by Mert et al. [16,17] show differences in air gap thicknesses between sitting and standing positions that change relative to localised body parts and directly influence the local thermal and evaporative resistance of a garment. Nonetheless, the impact of variations between body postures on the human thermo-physiology has not been investigated and the majority of authors provide the local clothing properties applicable only for the standing body position [18–25].

The most realistic method to determine local clothing thermal properties is the use of a thermal manikin with detailed body segmentation [5]. Nevertheless, the accessibility of this apparatus is restrictive on the account of the high costs of both the device and the necessity of additional equipment, including a climatic chamber. Therefore, other ways to obtain clothing properties can be found in the literature, which do not require specialised equipment. The most common approach is to choose a desired ensemble from an exhaustive database of clothing from standard ISO 9920 [18]. According to the definition of the *clo* unit, measured using a standing thermal manikin, all three clothing parameters are presented as global values for the whole-body (in essence virtual insulation covering the whole body) [18]. As a matter of fact, the uniform distribution yields unrealistic physiological responses, since the local extremes are averaged and the mean value is prescribed even for body parts without clothing in reality, typically face and hands [17,26]. To address this problem, Curlee [19] and Nelson et al. [23] developed a method to calculate local clothing parameters based on global parameters from McCullough et al. [24] and ISO 9920 [18] valid for 106 garments. This approach was presented only for single-layer clothing and the resolution of the model is limited to a single value for parts covered by the garment. Yet, there are obvious differences within air gaps, between some of the body parts considered by the model [16,17].

Another option is to estimate local clothing properties based on empirical formulae relating outdoor temperature and clothing insulation, such as the UTCI clothing model [20]. The data for the model was gathered from several independent studies on clothing habits of Europeans. The model has a resolution of 7 body segments, applicable for a standing person, and temperatures from approximately -30 °C to 32 °C [20]. The paper also presents compensation of thermal insulation for an increased airspeed.

Local air gap thickness mainly affects local clothing parameters and because of this, one of the emerging methods to precisely examine these parameters is three-dimensional (3D) body scanning. This al-

lows detailed assessment of the mean local air gap thicknesses, percentage of clothing contact area, and calculation of clothing area factors [27,28]. With the use of this information, prediction of thermal clothing insulation is possible based on basic laws of physics, using dedicated models for major body parts [29,30].

The optimal number of body segments for thermo-physiological modelling is conditioned by the specific application. The standard ISO 14505-2 [31] addresses cabin environments with seated positions and proposes segmentation of at least 16 body parts (11 parts if right-left symmetry is assumed for limbs) where distinct thermal conditions are expected, such as shade or a seat. Another standard ISO 15831 [32] recommends at least 15 segments (9 parts if right-left symmetry is assumed for limbs), and the most cited thermo-physiological models have similar resolutions to the ISO 15831 of up to 19 segments, with an additional spatial subdivision [33]. Similarly, the prevailing local thermal sensation models, such as models by Zhang [34,35], Jin [36], and Nilsson [37], have resolution covering major body parts of up to 13 segments assuming right-left symmetry. It is therefore reasonable to use a number of clothing segments equal to the number of segments of thermo-physiological and thermal sensation models to achieve the most realistic simulation of heat and mass transfer between the body and the environment.

Other parameters that are bound to the seated position are the thermal properties of the seat. Their determination requires specific instrumentation that can mimic contact pressure of a seated person, such as a seat tester STAN (Thermetrics, USA) [38] or a stamp tester as presented by Bartels [39]. The additional pressure is important because of the compression of seat layers, as well as the consequent changes in their thermal properties [39] and contact area with the body. Therefore, a measurement using a thermal manikin without realistic weight distribution and seat contact yields unrealistic results [40]. Values of additional thermal insulation provided by chairs were presented by McCullough et al.

[41] and Wu et al. [42], both used thermal manikins, however, without explaining whether and how the realistic contact was achieved.

The next parameter that is often neglected is the clothing fit and the associated air gap distribution, which influences resulting thermal and evaporative resistance [17]. Standard ISO 9920 recommends using clothing with normal fit, whereas ISO 14505 recommends tightly fitting clothing to get repeatable results. Thus, there is a need for an objective parameter that would describe fit of the clothing, for example, clothing ease allowance (*EA*) that is defined as a difference between girths of the body and clothing at given body landmarks. This parameter was found to be strongly correlated with air gap thickness, and hence, clothing thermal and evaporative resistance [21,27,43].

The aim of this study is to examine typical approaches of obtaining the local clothing thermal properties for simulations of physiological and perceptual responses with respect to their use in spatially heterogeneous conditions. Next, the focus is on differences between seated and standing body positions that to the best of our knowledge have not been addressed locally. The impact of the differences is shown by means of simulated thermo-physiological responses that are directly linked to thermal sensation. The application of the findings is in passenger transportation and a range of occupational settings, including but not limited to professional driving, machinery operation, and the office environment.

2 Methods

2.1 Study design

The study included the determination of clothing thermal properties for two clothing sets based on distinct approaches comprising measurement, modelling, and estimation of clothing properties. Thus, this study provides relevant information for laboratories following different approaches and with potential access to equipment listed in Table 1. *Cases 1* and *2* are assumed as references for sitting and standing positions, respectively, because of the state-of-the-art methods used. Moreover, the consistency of the methodology was achieved using the same clothing throughout the study.

Table 1 Overview of the examined cases and methods to determine clothing area factor (f_{cl}), intrinsic clothing insulation (I_{cl}), evaporative clothing resistance ($R_{e,cl}$). Right-left symmetry is assumed.

Case	f_{cl} (-)	I_{cl} ($m^2K.W^{-1}$)	$R_{e,cl}$ ($m^2Pa.W^{-1}$)	Position	No. of segments
1	3D scanning	Manikin heat loss method [32]	Manikin heat loss method [44]	sitting	13
2	Photography [18]	Manikin heat loss method [32]	Manikin heat loss method [44]	standing	13
3	Physical model [30,45]	Physical model [30,45]	Physical model [30,45]	sitting	8
4	Physical model [30,45]	Physical model [30,45]	Physical model [30,45]	standing	10
5	Regression model [21]	Regression model [21]	Physical model [30,45]	standing	11
6	ISO based model [23]; Tab. 1	ISO based model [23]; Tab. 1	ISO based model [19]; Appendix A	standing	3
7	ISO Database [18]; Tab. A.2	UTCI model [20]	ISO Database [18]; Formula 31	standing	7
8	ISO Database [18]; Tab. A.2	ISO Database [18]; Tab. A.2	ISO Database [18]; Formula 31	standing	1

The second part of the work is focused on the investigation of the sensitivity of the thermo-physiological model by Fiala [46] (FPCm5.3, Ergonsim, Germany) to changes in boundary clothing conditions. The model was chosen on a basis of its broad validation documentation [47–49]. The study focuses on the seated position in a neutral steady environment that is typical for a broad variety of indoor environments, and should serve as a benchmark for comparison of the eight individual approaches.

2.2 Definition of clothing sets and body positions for the study

The clothing sets included in this study represent typical indoor summer and winter clothing and were selected from the database of clothing presented by Psikuta et al. [27]. Most importantly, the focus was on the consistency of the clothing ease allowances (defined as the difference between the girth of clothing and a nude manikin at relevant body landmarks) throughout the study, as they affect resulting clothing area factor, thermal resistances, and evaporative resistances. The summer set consists of a collar shirt, light cotton jeans, briefs, short socks, and leather sneakers (Figure 1 B). The winter set was comprised of a turtle-neck shirt with a T-shirt worn underneath, heavier cotton jeans, leather shoes, as well as the same underwear as in the summer case (Figure 1 C). Detailed descriptions and the ease allowances of the clothing are given in Table 2.

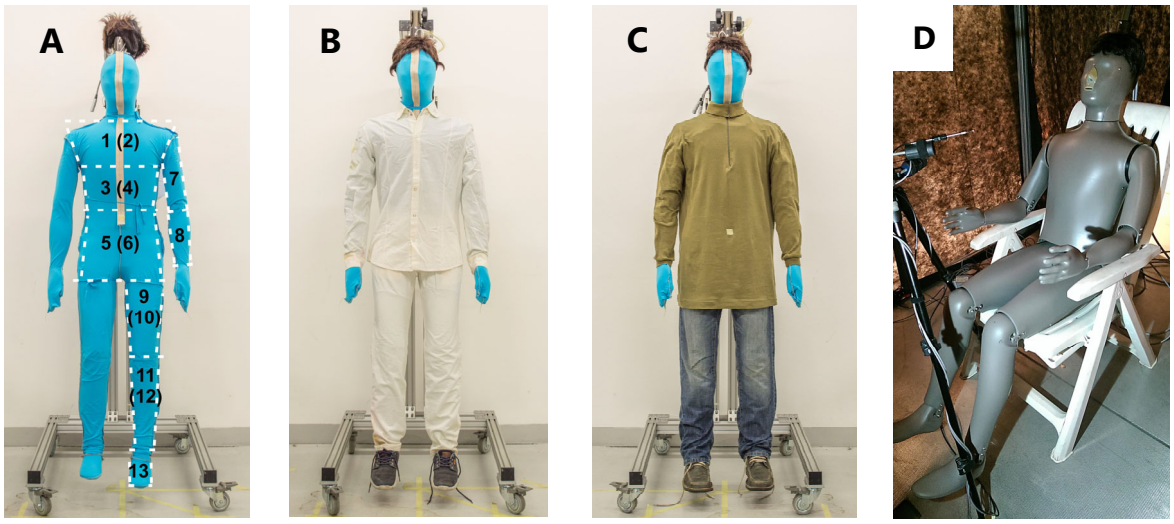

Figure 1 Illustration of the manikin used and the clothing sets applied. A – segmentation of a nude manikin with an artificial skin, posterior parts in brackets; B – summer indoor clothing; C – winter indoor clothing; D – seated position. *Note: segmentation from Figure 1A – 1 Chest, 2 Back, 3 Abdomen, 4 Lumbus, 5 Anterior pelvis, 6 Buttocks, 7 Upper arm, 8 Lower arm, 9 Anterior thigh, 10 Posterior thigh, 11 Shin, 12 Calf, 13 Foot.*

Table 2 Overview of clothing and *ease allowance (EA)* related to the size of a western type Newton thermal manikin.

	Indoor summer set			Indoor winter set				Both sets
Type	Smart shirt	Jeans light	Sneakers	Shirt	T-shirt	Jeans	Shoes	Briefs
Item in Psikuta et al. [27]	21	45	-	3	24	33	-	31
Fit	Regular	Regular	Regular	Regular	Regular	Loose	Regular	Regular
Fibre content (%)	100 CO	100 CO	Leather	100 CO	95 CO/5 EL	100 CO	Leather	100 CO
Specific weight (g/m^2)	137	179	Size	227	176	366	Size	145
Fabric structure	Plain weave	3/1 twill	EUR 42.5	Interlock	Single jersey	3/1 twill	EUR 42.5	1x1 rib

EA chest (cm)	14.5	-	-	10.5	11.5	-	-	-
EA waist (cm)	24.0	-	-	30.0	22.0	-	-	-
EA hips (cm)	13.0	8.0	-	12.0	10.0	14.0	-	-4.0
EA biceps (cm)	9.0	-	-	4.0	-	-	-	-
EA lower arm (cm)	8.0	-	-	2.5	-	-	-	-
EA thigh (cm)	-	6.0	-		-	3.0	-	-
EA lower leg (cm)	-	6.0	-	-	-	7.0	-	-

Notes: CO – cotton, EL – elastane.

A seating position typical of postures adopted for driving, operating of machinery, or office work, was adopted from the work of Mert et al. [28] in which an elbow angle of 120°, hip angle of 110°, and knee angle of 120° are specified (Figure 1D). The thermal manikin was seated on a plastic chair with openings accounting for approximately 40 % of its surface. The standing upright position with hands down (Figure 1) is typically reported in literature and was used to quantify the differences in comparison to the sitting position.

2.3 Case 1 – 3D scanning and heat loss method in seated position

The first studied case was considered as a reference case providing highest precision for determination of clothing thermal parameters in the seated position. The clothing area factor was measured by a 3D body scanning technique combined with post-processing software, which allows for the quantification of nude and dressed surface areas of individual body regions in a given position [17,27,50]. Details of the methodology and equipment were adopted from the study by Mert et al. [28]. The surface area was quantified four times for each clothing set, as well as for an undressed flexible manikin [28]. This manikin has, however, a different body geometry than the western Newton type thermal manikin (Thermetrics, USA) used to measure thermal and evaporative resistances. The differences in griths at given body land marks were typically of 2 cm, having the maximum of 6 cm at *Upper arm*. Linear interpolation was therefore used to compensate for the discrepancies between the manikins girths and consequently clothing ease allowances based on the clothing presented in Mert et al. [28]. This was

done according to the findings by Vesela et al. [21], where the linear relationship between the garment ease allowance and f_{cl} was demonstrated.

The local intrinsic clothing thermal (I_{cl}) and evaporative resistances ($R_{e,cl}$) were determined using the 34 zones Newton type manikin in a climatic chamber (detailed description of the chamber and the manikin in Fojtlín et al. [51]). The manikin was seated onto an adjustable plastic chair with perforation wearing the garments listed in Table 2. The 34 zones were merged into 13 segments (Figure 1A) to represent body segmentation of the Fiala model with resolution of upper and lower limbs, anterior and posterior torso. The measurement of both clothing sets and clothing resistances was executed three times independently, including dressing and undressing of the manikin.

The test conditions for the local intrinsic thermal resistances were adopted from ISO 15831 [32], which establishes requirements of a 34 °C manikin skin temperature, as well as air, mean ambient, and radiant temperatures of 24 °C, and relative humidity of 50 %. The air speed in the test was 0.1 ± 0.05 m/s that suits the target application in indoor environments with low air velocities. The calculation of the thermal resistances was done using the heat loss method according to Equation A.3a from ISO 15831 [32].

The evaporative clothing resistance was determined using a tightly fitting, long sleeve overall (Figure 1A) that was pre-wetted and worn only during evaporative resistance measurements [52,53]. The fabric for the overall was selected according to the recommendations from the study by Koelblen et al. [54] with thickness of 0.92 ± 0.03 mm, specific weight of 208 g/m, and fibre composition of 95 % cotton and 5 % elastane. The measurement was carried out at isothermal conditions of 34 °C (skin temperature equal to ambient temperature), relative humidity of 18 % (partial water vapour pressure of 957 Pa), and air speed of 0.1 ± 0.05 m/s. This setup allowed measurements in steady state conditions for at least 20 minutes to ensure reliable calculation of evaporative resistance. The calculation of evaporative resistance was done using the heat loss method described in ASTM F2370 [44].

2.4 Case 2 – photographic and heat loss method in standing position

Case 2 represents an example of experimental approach when an upright standing, non-articulated manikin (Figure 1A) and a camera are available. The methodology to determine I_{cl} and $R_{e,cl}$ is identical with *Case 1*, whilst the calculation of f_{cl} is based on superposition of photographs of nude and dressed manikin using graphical software (CorelDRAW X8, Corel Corporation, USA) according to the standard ISO 15831, Equation A7 [32]. In this case, the western Newton type thermal manikin was photographed using a full frame camera with a 35 mm lens placed 4.33 m in front of the manikin from four azimuth angles (front 0°, two side views 45°, 90°, and 180°) and a horizontal view of 0°. The standard [32] suggests using one additional horizontal angle of 60°, however, this was not feasible due to the ceiling clearance limitation of the laboratory. Although the original method was proposed to calculate the whole body f_{cl}, we divided the manikin's body into *Upper arm, Lower arm, Chest, Abdomen, Anterior hip, Back, Lumbus, Posterior hip, Upper leg, Lower leg, and Foot*, before determining their local values.

2.5 Cases 3 and 4 – analytical heat transfer model

Cases 3 and 4 represent one of the emerging methods to realistically and rapidly simulate f_{cl}, I_{cl}, *and* $R_{e,cl}$, taking the air gap thickness and contact area into account for a corresponding body part both in seated and standing positions. All three local clothing parameters were calculated using the in-house analytical clothing model developed at Empa [30,43]. The model exploits basic thermodynamic phenomena (conduction, radiation, and natural convection) and allows the calculation of local clothing parameters of multiple, layered garments. The physical model resolution is equal to the number of input parameters that were calculated according to the linear regression model proposed by Psikuta et al. [27] in *Case 4*. The model yields corresponding air gap thickness and contact area, in standing positions, based on the ease allowances of clothing (Table 2) for 14 body parts excluding feet. However, the upper and lower chest as well as upper and lower back were averaged (area weighed) into two re-

spective body parts to match the segmentation in Figure 1A and the body resolution of the thermal manikin.

In *Case 3*, the resolution of the model was reduced to eight parts, since the four body parts in contact with the seat were not considered. The air gap thickness and contact area were taken from the database of garments in the seated position by Mert et al. [16] (positions U5, L4). The air gap thickness and contact area were obtained by linear interpolation based on the ease allowances.

2.6 Case 5 – regression and analytical heat transfer models

Case 5 represents an approach based on predictions of local f_{cl} and I_{cl} on clothing ease allowances proposed by Vesela et al. [21]. This allows simple calculation of the clothing properties based on readily available parameters. The regression models were derived from single layer garments in standing position. Yet, the behaviour of the multilayer clothing was described in the study by Mark et al. [55] using the 3D scanning technique. The main findings indicate that the inner layer is negligibly influenced by the outer layer as long as the ease allowance of the outer layer is bigger than that of the inner one. Further, for the majority of casual clothing, it can be assumed that the representative f_{cl} and I_{cl} can be calculated according to the ease allowances of the outer garment, and was also performed in this study. The overview of the ease allowances is given in Table 2. The methodology to calculate $R_{e,cl}$ was not presented in the study by Vesela et al. [21] and was adopted from *Case 4* [30].

2.7 Case 6 – ISO 9920 based model

Curlee [19] and Nelson et al. [23] developed a method to calculate all three local clothing parameters valid for 106 garments from McCullough et al. [24] and ISO 9920 [18]. However, the resolution of the algorithm is limited to individual clothing items covering given body parts, such as a shirt covering the whole torso and arms. As the method does not clarify an approach to calculating the resistances of multiple, layered garments lying atop one-another, the clothing resistances were instead totalled to match the procedure of Vesela et al. [11]. The clothing area factors of the outer layers were calculated as described in section 2.6.

Following clothing was selected for this study from Appendix A [19]:

- Summer clothing: Long sleeve collar shirt (broadcloth); Straight long fitted trousers (denim); Soft soled athletic shoes; Calf length dress socks.
- Winter clothing: Long-sleeve turtleneck (thin knit); Short sleeve collar shirt (broadcloth); Straight long lose trousers (denim); Hard soled athletic shoes; Calf length dress socks.

2.8 Case 7 – empirical model

The UTCI clothing model predicts local thermal insulation for 7 body parts (head, torso with upper arms, lower arms, hands, upper legs, lower legs, feet) [20]. Despite the model's focus on outdoor applications, we assumed similar clothing preferences for indoor and outdoor environments based on two mild ambient temperatures of 24 °C (summer indoor clothing) and 21 °C (winter indoor clothing). These two temperatures were defined according to the PMV-PPD thermal sensation model described in the ISO 7730:2005 [56] as a thermo-neutral environment for activity level representing office work or driving at 1.3 met, clothing insulation according to ISO 9920 of 0.62 (summer) and 1.01 clo (winter), and air speed of 0.1 m/s.

2.9 Case 8 – estimation based on ISO 9920

Standard ISO 9920 [18] provides an exhaustive list of civil, working, and non-western clothing properties determined by a standing thermal manikin. Therefore, this approach is of main interest for a variety of engineering applications where there is no dedicated equipment available. The I_{cl} and f_{cl} are presented as a resultant insulation prescribed to all body parts, even to those parts, which are not covered by the clothing in reality. Similarly, the $R_{e,cl}$ was calculated as a whole body value according to Equation 31 from the standard [18] as intrinsic thermal insulation multiplied by a constant of 0.18.

Two clothing sets were selected from the standard (Table A.2) [18] based on the closest match of the description of the garments as follows:

- Summer clothing: *Ensemble 108* – briefs, long-sleeve shirt, fitted, trousers, calf-length socks, shoes.
- Winter clothing: *Ensemble 114* – briefs, T-shirt, shirt, loose trousers, round-neck sweater, calf-length socks, shoes.

2.10 Determination of seat thermal properties

As a consequence of the seat, the body segments in contact with it experience increased thermal and water vapour resistances. Direct measurement of these parameters with the Newton type manikin is not accurate because of the manikin's rigid body construction and low body weight, which inhibit the resulting contact area from imitating the interaction of a representative body and seat [40]. As a result, lower compression of seat layers and smaller contact area with differences in shape are expected for manikins when comparing to humans. For this reason, the corresponding data was adopted from the study on aeroplane seats with similar construction to automotive seats, with moulded foam cushioning and leather cover. Using a stamp tester, a thermal resistance of 0.55 m^2K/W (Fig. 7 in [39]) was measured for the seat, whilst an evaporative resistance of 100 m^2Pa/W [39] was determined using the same seat in human trials. Finally, we estimated the seat clothing area factor to be 2.0 units based on the dimensions of the seat.

2.11 Thermo-physiological simulations

Benchmark tests of clothing thermal properties are helpful in the development and evaluation of clothing systems, but thermo-physiological responses do not show a similar sensitivity to clothing properties as can be detected by benchmark tests [48]. Therefore, the eight studied cases were used as separate inputs for thermo-physiological modelling under the same environmental conditions to quantify the resulting differences in physiological responses among the methods.

To do so, two setups corresponding to summer (t_{air} = t_{rad} = 24 °) and winter (t_{air} = t_{rad} = 21 °) indoor environments with an ambient air speed of 0.1 m/s, and relative humidity of 50 % were carried out using the broadly validated Fiala model FPCm 5.3 [46]. The metabolic production of 1.3 met was select-

ed from a database presented by Ainsworth et al. [57] as an average from reading, typing, and driving. The simulations were run for 4 hours with a 5 minutes simulation interval to reveal the development of thermo-physiological response in a long steady exposure.

In the simulations, the clothing thermal properties of shoes were obtained from *Case 2 and* considered in f_{cl} for *Cases 1,3,4,5*, I_{cl} for *Cases 3,4,5*, and $R_{e,cl}$ for *Cases 3,4,5,6*. Additionally, the simulations account for the thermal effects of the seat (Section 2.10). The seats were applied as the clothing boundary conditions to posterior thighs, posterior hip, posterior abdomen, and posterior thorax of the virtual humanoid according to the findings from Fojtlín et al. [40]. This was done for *Cases 1* to *7*, whereas the eighth case was executed according to the directions from ISO 9920 [18], such that an additional thermal insulation of 0.039 $m^2K.W^{-1}$ was added to the whole-body resistance. As the standard does not clarify how to treat f_{cl} and $R_{e,cl,}$ the values were unchanged for *Case 8* in the standing position.

Firstly, to assess the effects of clothing boundary conditions, we examined mean skin and rectal temperatures to provide a global overview of the body thermal state. Secondly, the cumulative sweating was investigated to quantify the amount of liquid sweat excreted from the whole body. Next, to measure the development of local parameters, skin temperatures were examined at Chest and Anterior thighs, which were selected because of their dominant surface area that is not in the contact with the seat and their distinct susceptibility to change air gap thickness with the change of position. Furthermore, dynamic thermal sensation (*DTS*) was calculated to predict whole body thermal sensation on the 7-point scale ranging from - *3 Cold*, through *0 Neutral*, to *3 Hot* [56]. Finally, skin wettedness was examined at *Chest* and can be considered as a perception of wet discomfort being physically defined as the ratio of the actual sweat rate to the potentially evaporating amount of sweat.

3 Results

3.1 Comparison of the methods

Local clothing properties f_{cl}, I_{cl}, and $R_{e,cl}$ were divided into four groups of body parts, namely anterior and posterior torso, and upper and lower limbs (Figures 2 and 3). Furthermore, Figures 2 and 3 show the local clothing properties obtained from all examined methods for a given body part in one plot. A result from one body part is connected with a dashed line for easier tracking of its development depending on the method. The results from methods having body parts resolutions lower than the reference (13) were either left blank, if missing, or presented as one value for related body parts, for instance lower leg from UTCI model [20] covers *Shin* and *Calf*. Where applicable in Figures 2 and 3, error bars represent standard deviation of the repeated measurements. The differences between repeated manikin measurements in I_{cl} fell within the recommended 4 % [32], thus, the standard deviation was too small to be visualised and was not plotted. Despite the anatomically unrealistic contact of the manikin with the seat [40], the I_{cl} and $R_{e,cl}$ from the contact area in *Case 1* (Figures 2 and 3 – *Back, Lumbus, Buttocks, and Anterior thighs*) are shown for full overview. Because of the limitations of the 3D scanning method in the contact area, in *Case 3*, the f_{cl} was calculated based on an increase of the skin surface area by the thickness of the fabrics. As reference body geometry we used a virtual humanoid from the Fiala thermo-physiological model [46]. Further, the I_{cl} and $R_{e,cl}$ was estimated as thermal and evaporative resistances of the fabrics only.

Assuming that *Case 1* (manikin measurement in seated position) is the most accurate method, the variation between all the methods for both clothing ensembles was as follows:

- 13 – 43 % of the reference value for clothing area factor (f_{cl}) depending on body part;
- 35 – 198 % of the reference value for intrinsic thermal insulation (I_{cl}) depending on body part;
- 53 – 233 % of the reference value for intrinsic evaporative resistance ($R_{e,cl}$) depending on body part.

These variations were found to be very similar for both clothing ensembles with somewhat higher values for the looser, multilayer winter ensemble (Figures 2 and 3). When comparing 6 cases based on standing body position only (*Cases 2, 4, 5, 6, 7,* and *8*, Table 1), their variation was as follows:

- 6 – 36 % of the reference value for clothing area factor (f_{cl}) depending on body part;
- 32 – 204 % of the reference value for intrinsic thermal insulation (I_{cl}) depending on body part;
- 45 – 232 % of the reference value for intrinsic evaporative resistance ($R_{e,cl}$) depending on body part.

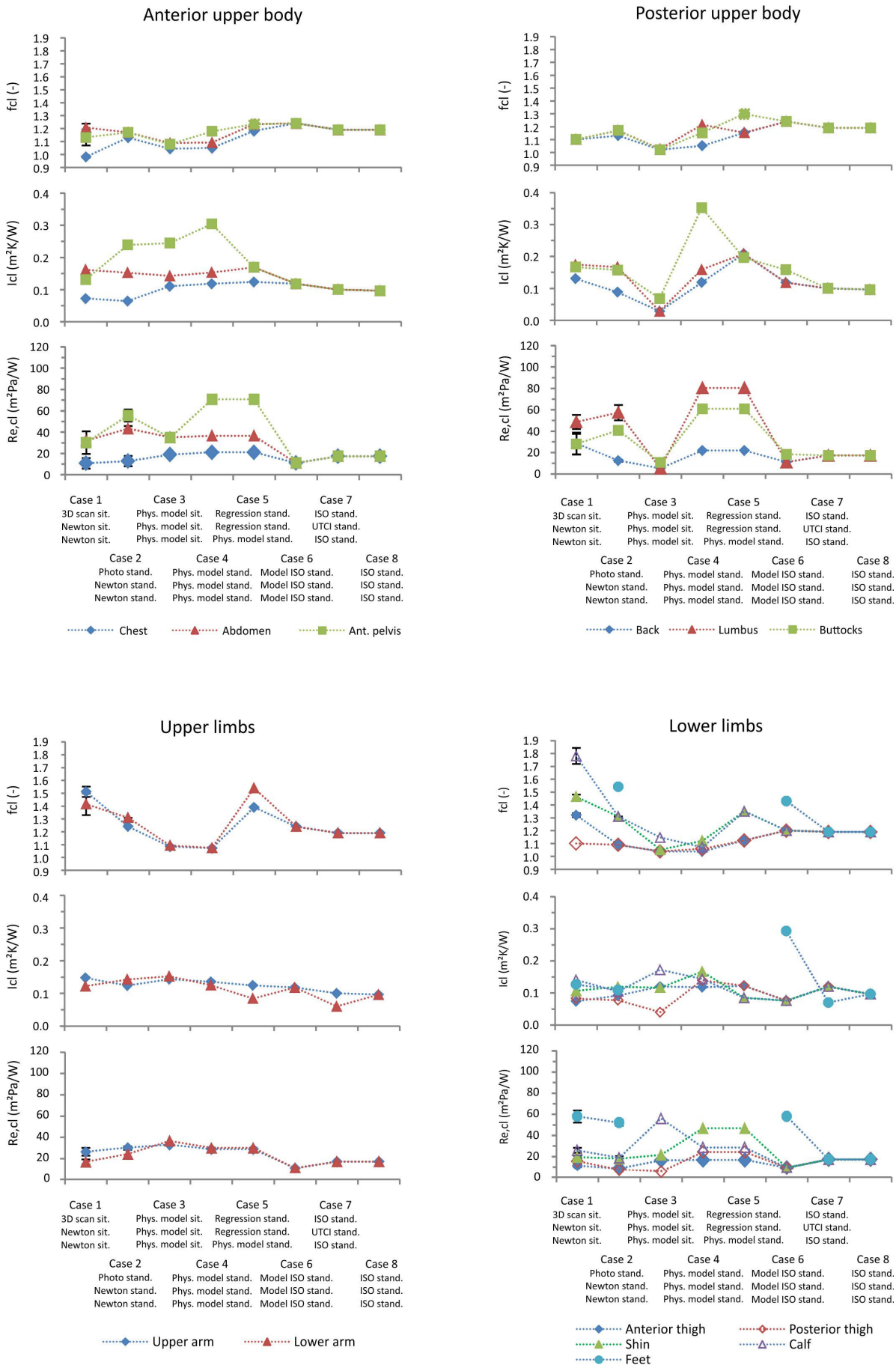

Figure 2 The clothing thermal properties of the summer indoor clothing set shown for 13 body parts excluding the seat thermal properties. Error bars depict standard deviation.

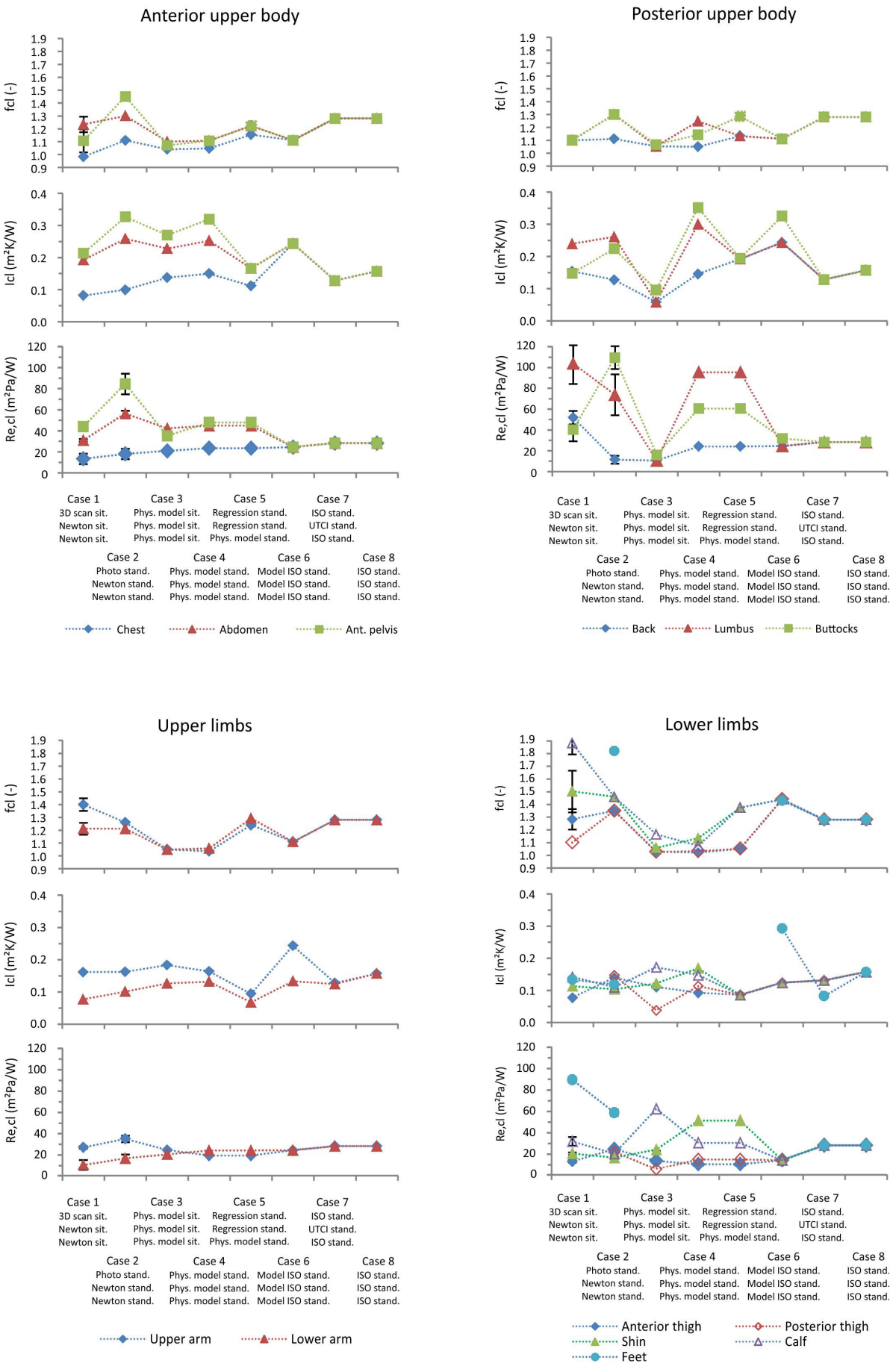

Figure 3 The clothing thermal properties of the winter indoor clothing set shown for 13 body parts excluding the seat thermal properties. Error bars depict standard deviation.

3.2 Differences in manikin measurements between sitting and standing body positions

The differences between parameters for both sitting and standing positions are depicted in Figure 4 for selected representative body parts with and without a major change in their orientation. The body parts in contact with the seat were considered without the seat thermal insulation. The following difference margins between sitting and standing positions were found, namely:

- up to 31 % of the reference value (*Case 1*) for f_{cl} depending on body part;
- up to 80 % of the reference value (*Case 1*) for I_{cl} depending on body part;
- and up to 92 % of the reference value (*Case 1*) for $R_{e,cl}$ depending on body part.

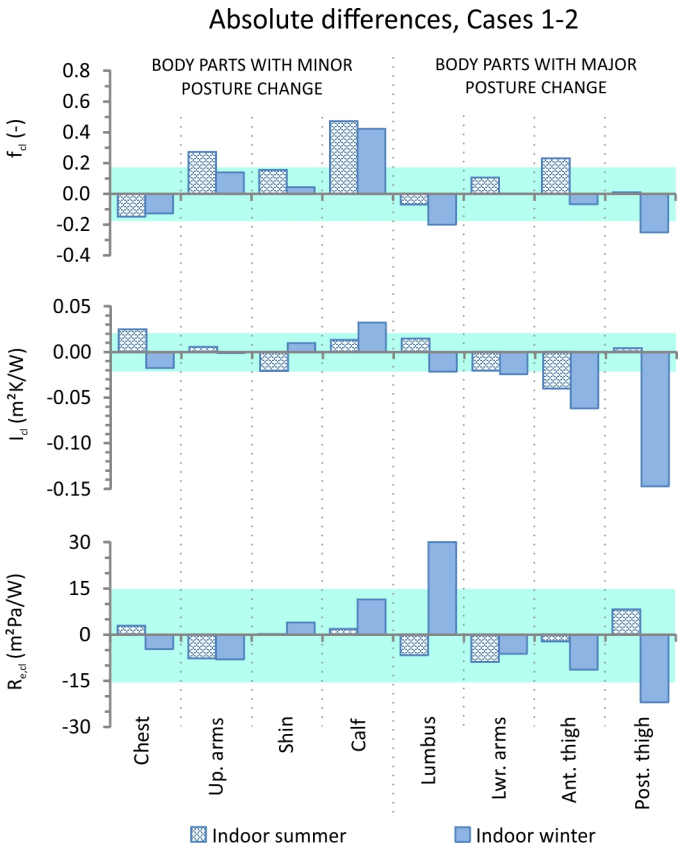

Figure 4 Absolute differences between clothing thermal properties between the positions (Cases 1-2) for summer and winter indoor clothing, respectively. The transparent field depicts a range of three standard deviations of the methods used in Case 1 covering 99.7 % of observations being ± 0.17 units for f_{cl}, ± 0.02 m²K/W for I_{cl}, and ± 15 m²Pa/W for $R_{e,cl}$.

3.3 Effects of the clothing and body position on thermo-physiology

The results for the whole-body and local thermal responses from thermo-physiological simulations are depicted in Figure 5, separately for summer and winter scenarios. In total, eight responses were plotted such as mean skin temperature, rectal temperature, skin temperature at chest, skin temperature anterior thigh, cumulative sweating, dynamic thermal sensation (DTS), and skin wettedness at *Chest*. Each line represents a development of a given simulated response corresponding to one of the examined methods to determine the clothing properties. To differentiate between sitting and standing body positions, the sitting positions are represented within the plots by continuous lines, whilst standing positions are denoted by dashed lines.

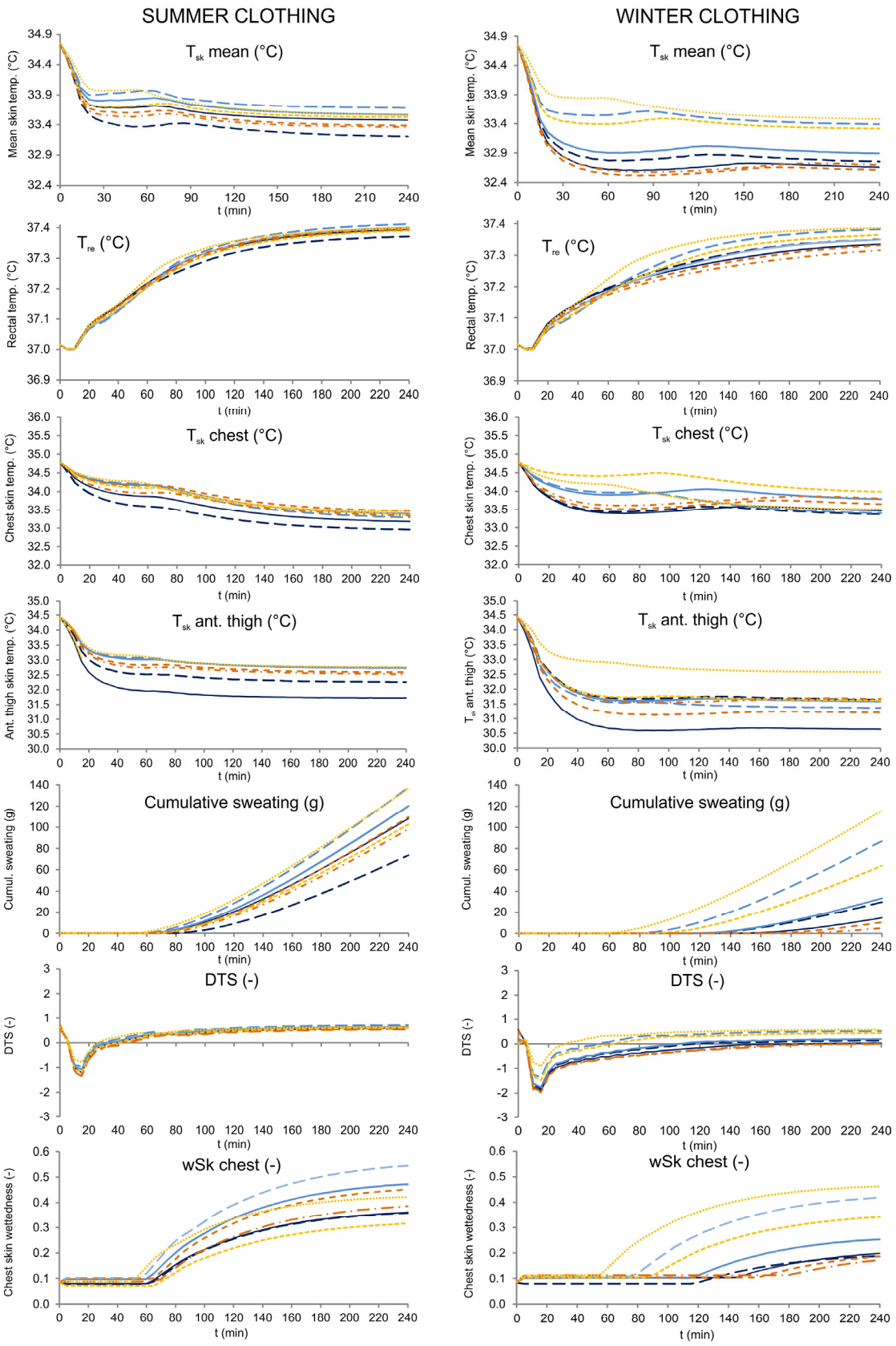

Figure 5 Results of the thermo-physiological simulations separately for summer and winter clothing.

4 Discussion

4.1 Comparison of the methods

In this study, we compared six various methods to obtain clothing area factor, seven methods for intrinsic thermal insulation, and five methods for intrinsic evaporative resistance determination. These methods were combined into eight distinct cases corresponding to different availabilities of advanced equipment to determine the clothing properties in an exemplary laboratory. In theory, all the examined methods should yield the same results. Contrary to this, large differences of more than 200% were found for all three clothing parameters and body parts covered by the clothing (Figures 2 and 3) assuming that *Case 1* (manikin measurement in seated position) is the most accurate reference method (13 – 43 %, 35 – 198 %, and 53 – 233 % of the reference value for clothing area factor (f_{cl}), intrinsic thermal insulation (I_{cl}) and intrinsic evaporative resistance ($R_{e,cl}$), respectively, depending on body part).

It is worth to mention that this variation cannot be predominantly attributed to the body position. When comparing 6 cases based on standing body position only (*Cases 2, 4, 5, 6, 7,* and *8*, Table 1), their variation was slightly lower, such as 6 – 36 %, 32 – 204 %, and 45 – 232 % of the reference value for clothing area factor, intrinsic thermal insulation, and evaporative resistance, respectively, depending on body part.

The error in f_{cl} was greater at the limbs (0.16 – 0.81 units of difference among the methods) than at the torso (0.15 – 0.38 units of difference among the methods). The median of error among all cases was 0.36 units, whereas the most outstanding difference was observed at calves of up to 0.81 units (Figure 3, *Case 3*). Here, the method assumes a cylinder as a base shape wrapped by clothing which includes the average air gap thickness. This does not fully represent the real situation of the hanging trouser leg in the sitting position. Regarding I_{cl} and $R_{e,cl}$, amongst the methods tested the upper limbs presented the best matching predictions, re-

sulting in differences of 0.05 – 0.15 m^2K/W and 15.8 – 25.7 m^2Pa/W, respectively. The rest of the body parts did not show any clear trends in prediction accuracy, having average differences among the methods in I_{cl} and $R_{e,cl}$ of 0.14 m^2K/W and 38.8 m^2Pa/W respectively, with the greatest span of predictions of 0.2 m^2K/W in I_{cl} and of 60.1 m^2Pa/W in $R_{e,cl}$ at *Anterior pelvis*.

The predictions of all clothing parameters were the most realistic in *Cases 3, 4,* and *5* compared to the reference values from *Case 1*. Presumably, the rest of the methods poorly capture changes in the clothing parameters because of their limited body resolution. *Cases 1* and *2* were carried out with resolutions of 13 segments as well as *Cases 3, 4,* and *5,* whereas the methods used in *Cases 6, 7,* and *8* work with body segmentation of three, seven, and one components, respectively. Thus, distinct body parts (such as *Chest*, *Abdomen*, *Ant. Pelvis, Back, Lumbus, and Arms* in *Case 6*) are lumped into one segment that yields an averaged value in *Case 6* of 0.12 m^2K/W for summer clothing and of 0.24 m^2K/W for winter clothing when neglecting local extremes. Area weighted average from the same segments from the more detailed *Case 2* shows comparable results of 0.15 m^2K/W and 0.20 m^2K/W in summer and winter clothing, respectively. At the same time, the local values in *Case 2* differ substantially from their average, with extremes at *Chest* and *Anterior Pelvis* of 0.06 m^2K/W and 0.24 m^2K/W for summer clothing and of 0.10 m^2K/W and 0.33 m^2K/W for winter clothing, respectively. Therefore, it is essential to account for local extremes.

4.2 Differences in manikin measurements between sitting and standing positions (*Cases 1* and *2*)

The change of body position implies a change in orientation for several regions of the body to varying extents. This is particularly evident when one considers the significant degree of thigh reorientation, when contrasted to the minor reorientation of the chest when moving between standing and sitting positions. The differences in all three clothing thermal properties for both positions were found and are depicted in Figure 4 for selected representative body parts with

and without a major change in their orientation. The least pronounced deviations (of up to 31 %) were discovered in f_{cl}. Despite slight postural changes at *Calf* and *Upper arm*, here, an error in f_{cl} was three standard deviations higher than of other typical measurements (Figure 4).

Although minor variations would be expected due to slight postural changes, it was found that the an error in f_{cl} at the *Calf* and *Upper arm* was three standard deviations higher than of other typical measurements. Despite minor changes were expected only because of the minor posture change, we found the opposite in f_{cl} at the *Calf* and *Upper arm*, being higher than three standard deviations of typical measurement (Figure 5). The error at *Calf* can be explained by the hanging trouser leg in the seated position yielding a difference of approximately 0.5 f_{cl} units. The discrepancy at *Upper arm* is plausibly related to methodological differences between *Cases 1* and *2*.

The photographic method is based on the projection of a three-dimensional object to a two-dimensional plane. Whilst there is an expected loss of detail in the clothing topography through this approach in C*ase 2*, the 3D scanning method of *Case 1* accounts for clothing folds which affect total clothing surface area. Thus, the error between the scanning and the photography is of 0.28 f_{cl} units for summer and 0.12 f_{cl} units for winter clothing. However, it is difficult to generalise the methodological error because the number and the size of the folds vary over the body surface. Next, in the sitting position, the 3D scanning method yields f_{cl} at *Chest* lower than 1 as opposed to the photographic method. The probable reason for this is the anatomic curvature of the flexible manikin's chest [16] that has a greater surface area than the stretched flat garment that covers the chest, whereas the Newton thermal manikin (*Case 2*) has simplified concave chest curvature. Thus, its skin surface is smaller than the surface of the outer garment yielding f_{cl} greater than 1.

The results in I_{cl} and $R_{e,cl}$ from *Cases 1* and *2* exhibit greater variation (of up to 80% and 92 %, respectively) and correspond to a redistribution of the mean air gap thicknesses between the positions reported by Mert at al. [28], and its consequent impact on thermal and evaporative resistances as reported by Psikuta et al. [45]. In compliance with these two studies, we found decrease in I_{cl} and $R_{e,cl}$ greater than three standard deviations of measurement at *Anterior pelvis*, *Anterior thighs*, *Abdomen,* and *Lower arm* (Figure 4). At these parts, air gaps collapse and the I_{cl} of two-layer winter clothing might be equalled to standing summer clothing. This underlines the importance of distinguishing between the body orientations and using local values.

4.3 Effects of the clothing and position on thermo-physiology

Differences in local clothing properties may be integrated by human thermoregulation and, thus, result in minimal discrepancy of global parameters such as mean skin or core temperatures. The variation of mean skin temperatures among the eight methods was within 0.6 and 1.3 °C in summer and winter clothing, respectively. This rather remarkable error can be related to a considerable change in local thermal sensation from approximately 0.5 to 1.5 units, depending on the thermal sensation model, and its scale as demonstrated by Koelblen and Veselá et al. [11,58]. However, the differences between the body positions were marginal within 0.3 °C. Finally, we found minor impact of the eight clothing inputs on the predicted rectal temperature of less than 0.1 °C.

The local thermo-physiological parameters show substantial variation that corresponds to variation in the clothing inputs even if applied in a neutral, steady, and uniform environment (Figure 5). In reference to *Case 1*, the approaches whose results which most closely matched were found to be the same as in the investigation on the clothing thermal properties, namely *Case 3* (modelling based on air gap thicknesses in sitting) and *Case 5* (regression model based on air gap thickness). The worst performing approach was *Case 8* based on the whole-body estima-

tion of clothing parameters and the ISO based model from *Case 6* (Figure 5). It seems to be not possible to recover any local data based on whole body values with reasonable accuracy when local data is necessary, as shown by performance of *Case 6*.

Next, the development of the local skin temperatures is clearly affected by the variation of local clothing thermal properties. For instance, relatively low differences in the clothing properties at *Chest* (Figures 2, 3 and 5) result in the absolute differences in skin temperatures of 0.5 °C among all methods and of 0.2 °C between the body positions (Figure 5). On the contrary, higher variability of input parameters, such as at *Anterior thighs*, leads to a spread of the predicted local skin temperature of 1 and 2 °C in summer and winter clothing, respectively. Next, cumulative sweating indicates low to mild sweat excretion that amounts between 5 g (*Case 7* winter clothing) and 138 g (*Case 4* summer clothing). The onset of sweating varied substantially in the winter clothing between 60th (*Case 8*) and 190th minute (*Case 7*).

The precise predictions of the sweat amount and onset of sweating can enhance a proper prediction of skin wettedness linked to so-called wet discomfort from sweating. At the end of the exposure, this parameter ranged from 0.03 to 0.61 and from 0.06 to 0.71 in summer and winter clothing, respectively. The highest values were always found in the contact parts with the seat and the lowest for bare body parts, such as hands. The variability of predictions can be demonstrated on *Chest*, where the threshold for discomfort of 0.42 units [59] was exceeded in the winter clothing tests of *Cases 4* and *8* (value reached in 210 min and 145 min, respectively), and in the summer clothing *Cases 3* (125 min)*, 4, 5,* and *8* (185 min). The threshold was not reached in the *Cases 1* and *2* (Figure 5).

Although, the examined deviations in thermo-physiological parameters are not critical in regards to medical relevance, such as uncompensated heat storage or dehydration, they nega-

tively influence accuracy of thermal sensation prediction. The benchmark value for the assessment of thermal sensation was adopted from ISO 7730 [56] as ±0.5 units (thermal environment category B corresponding to less than 10 % of dissatisfied occupants with the thermal environment). The whole-body thermal sensation index *DTS* showed minor variations between the methods which was within 0.2 units for summer clothing and significant discrepancies were found in the winter scenario of up to 0.6 units (*Cases 4, 7, 8* compared to *Case 1*, Figure 5). Yet, the contribution of the position change, demonstrated in *Cases 1* and *2*, did not reveal any significant differences in *DTS* (below 0.1 units). However, it can be expected to see major differences in the local thermal sensation predictions.

The whole body values are not sufficient for local modelling and the seated posture induces a drop in thermal and evaporative resistance due to collapse of air layers underneath the clothing. Furthermore, the previously discussed variability of the thermo-physiological responses induced by the clothing inputs urges the use of precise local clothing parameters. Only then with these parameters can reliable simulations of thermo-physiological responses be conducted. In addition, the discrepancies between the predictions may inflate for conditions further away from thermo-neutrality and cause even larger errors in predictions of thermal sensation, comfort or performance of the occupants [58,60]. This applies for instance in free running buildings with a larger temperature range, vehicles, and industrial spaces with special conditioning due to technological processes.

4.4 Sensitivity analysis

In order to examine the sensitivity of the physiological response to variations in clothing parameter inputs, we reproduced the winter case using upper and lower extremes of the clothing parameters out of the 8 cases. Only one clothing parameter was changed at a time (for instance f_{cl}) while keeping the rest (in this case I_{cl} and $R_{e,cl}$) as the reference – *Case 1* sitting.

The results are displayed in Figure 6 and clearly show the variability of I_{cl} inducing the greatest effect on all monitored thermo-physiological parameters in thermo-neutral environmental conditions (Details in *Section 2.11*). Differences in skin temperatures and *DTS* exceeded 1 °C and 1 unit, respectively. As previously discussed, such discrepancies have measurable impact on the perceived thermal sensation and/or comfort. Despite high deviations in f_{cl} (up to 43 %) and $R_{e,cl}$ (up to 233 %), the effect of these two parameters on thermo-physiology is practically negligible. However, it can be expected that the importance of $R_{e,cl}$ in warm conditions will play a more significant role, as a larger amount of sweat is excreted and needs to be transported through the clothing system. Secondly, the variation of $R_{e,cl}$ between methods might be larger when protective clothing with higher evaporative resistance is considered, since this clothing is less represented and more difficult to unambiguously identify in databases used in regression and reference table methods.

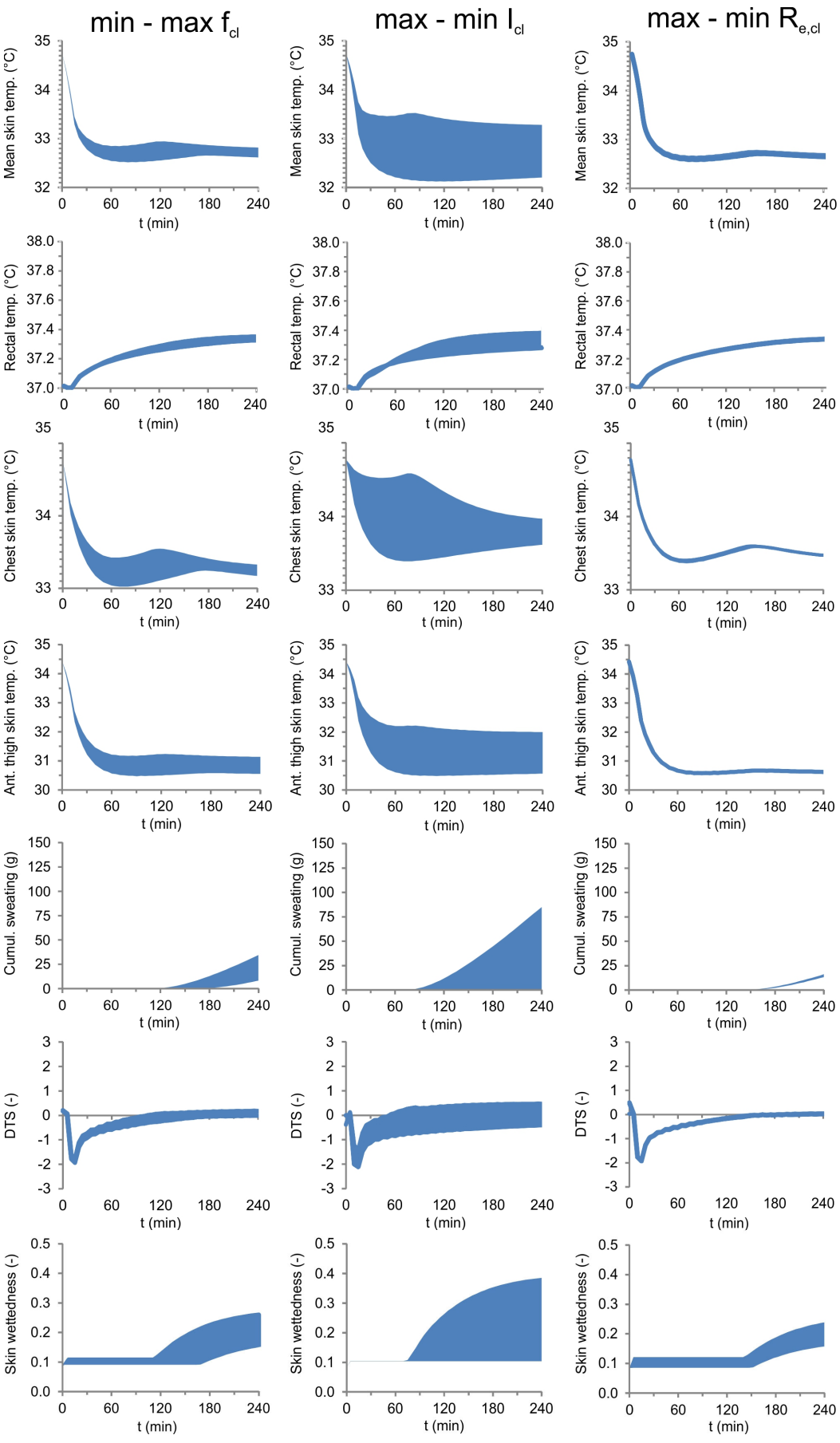

Figure 6 Sensitivity of thermo-physiological responses to changes in individual clothing parameters.

4.5 Reliability of the reference methods

Despite using the state-of-the-art methods as a reference, several remarks should be noted on their reliability. Firstly, the precision of 3D scanning method – used in this study to determine clothing area factor – is typically better than 1.7 mm [28,61]. Based on the dimensions of the passive body geometry in the Fiala model [46], an addition of 1.7 mm to the body part radius causes a change in f_{cl} as low as 0.01 units. This increment is, thus, negligible compared to observed f_{cl} variation between examined methods and we conclude high reliability of this method. Secondly, the measurement of I_{cl} has the typical error among the repeated measurements of less than 4 % that is recommended by the standard ISO 15831 [32]. The only two local extremes of 10 % were found at the *Abdomen* and *Back*. Finally, the precision of the methodology to determine $R_{e,cl}$ has several methodological limitations that are bound to complexity of the heat and mass transfer through the garment, such as heat pipe effect, wicking, partial drying, wet conduction [62], evaporative heat energy taken from the environment [53], and inability to control the temperature of the wetted manikin's skin [63,64]. Thus, the skin temperature might be lower than assumed and introduce an error in $R_{e,cl}$ of up to 14% [63]. Nevertheless, according to our sensitivity analysis in mild thermal environments, the errors in $R_{e,cl}$ have only a minor impact on the physiological response.

5 Conclusions

Eight typical approaches to determine clothing properties for thermo-physiological and thermal sensation predictions were examined, both in sitting and standing body positions, using two sets of indoor clothing. Considerable differences among the eight examined methods in clothing area factor, intrinsic clothing thermal insulation, and evaporative resistance were found. Next, the findings from the study also confirm a need to differentiate between the local clothing inputs in seated and standing positions and urge to avoid using the whole body val-

ues that are not sufficient for local thermo-physiological modelling. The impact of the variation of the clothing parameters was shown in the simulations of physiological responses in thermo-neutral, homogeneous, and steady conditions. Consequently, due to differences in the clothing inputs, we found major deviations of skin temperatures, skin wettedness, and global thermal sensation votes. Furthermore, sensitivity analysis revealed a dominant influence of intrinsic clothing thermal insulation on the simulated responses, while clothing area factor and evaporative resistance had minor influences. Therefore, we recommend using the highest precision method available to determine I_{cl}, such as a manikin measurement, physical modelling or regression modelling. Nonetheless, it can be expected that discrepancies among the methods will be stressed out in heterogeneous and extreme ambient conditions, for instance in vehicular cabins exposed to hot or cold weather conditions, free running buildings or specific working environments.

The findings from this study are beneficial for a broad variety of research and engineering applications, where a design of a thermal environment is essential to ensure comfort and performance of the occupants, such as multiple sitting occupations (office work, assembly or sewing work, driving) and passenger transportation. Here, the acceleration of innovation cycles and reduction of costs for physical studies is advanced by the selection and use of reliable thermo-physiological models, which incorporate realistic clothing boundary conditions whilst also accounting for body position.

6 Acknowledgements

The part of work conducted at Empa was supported by the [HEAT-SHIELD project within EU Horizon 2020 program] under Grand [RIA 668786-1]. The experimental part of the work conducted at Brno University of Technology was supported by the [Ministry of Education project Youth and Sports of the Czech Republic] under the "National Sustainability Programme I"

[LO1202 Netme Centre Plus]; and the [Brno University of Technology] under the project Reg. No. [FSI-S-17-4444]. The authors would like to thank Ankit Joshi from Empa, St. Gallen for help with calculating clothing thermal properties in *Cases 3 and 4*.

7 References

[1] M. Veselý, W. Zeiler, Personalized conditioning and its impact on thermal comfort and energy performance - A review, Renew. Sustain. Energy Rev. 34 (2014) 401–408. doi:10.1016/j.rser.2014.03.024.

[2] M. Veselý, P. Molenaar, M. Vos, R. Li, W. Zeiler, Personalized heating – Comparison of heaters and control modes, Build. Environ. 112 (2017) 223–232. doi:10.1016/j.buildenv.2016.11.036.

[3] W. Pasut, H. Zhang, E. Arens, Y. Zhai, Energy-efficient comfort with a heated/cooled chair: Results from human subject tests, Build. Environ. 84 (2015) 10–21. doi:10.1016/j.buildenv.2014.10.026.

[4] M. Luo, E. Arens, H. Zhang, A. Ghahramani, Z. Wang, Thermal comfort evaluated for combinations of energy-efficient personal heating and cooling devices, Build. Environ. 143 (2018) 206–216. doi:10.1016/j.buildenv.2018.07.008.

[5] A. Psikuta, J. Allegrini, B. Koelblen, A. Bogdan, S. Annaheim, N. Martínez, D. Derome, J. Carmeliet, R.M. Rossi, Thermal manikins controlled by human thermoregulation models for energy efficiency and thermal comfort research – A review, Renew. Sustain. Energy Rev. 78 (2017) 1315–1330. doi:10.1016/J.RSER.2017.04.115.

[6] E. Foda, K. Sirén, Design strategy for maximizing the energy-efficiency of a localized floor-heating system using a thermal manikin with human thermoregulatory control, Energy Build. 51 (2012) 111–121. doi:10.1016/j.enbuild.2012.04.019.

[7] D. Fiala, A. Psikuta, G. Jendritzky, S. Paulke, D.A. Nelson, W.D. van Marken Lichtenbelt, A.J.H. Frijns, Physiological modeling for technical, clinical and research applications, Front. Biosci. S2. (2010) 939–968.

[8] C. Huizenga, Z. Hui, E. Arens, A model of human physiology and comfort for assessing complex thermal environments, Build. Environ. 36 (2001) 691–699. doi:10.1016/S0360-1323(00)00061-5.

[9] M. Hepokoski, A. Curran, D. Dubiel, Improving the accuracy of physiological response in segmental models of human thermoregulation, in: S. Kounalakis, M. Koskolou (Eds.), XIV Int. Conf. Environemntal Ergon. Nafplio, Nafplio, 2011: pp. 102–103. https://www.researchgate.net/profile/Petros_Botonis/publication/270647588_THE_EFFECT_OF_SKIN_SURFACE_MENTHOL_APPLICATION_ON_RECTAL_TEMPERATURE_DURING_PROLONGED_IMMERSION_IN_COOL_AND_COLD_WATER/links/54b199fb0cf220c63cd12836.pdf#page=360.

[10] B. Koelblen, A. Psikuta, A. Bogdan, S. Annaheim, R.M. Rossi, Thermal sensation models: A systematic comparison, Indoor Air. 27 (2016) 1–10. doi:10.1111/ina.12329.

[11] S. Veselá, B.R.; Kingma, A.J. Frijns, Local thermal sensation modeling: a review on the necessity and availability of local clothing properties and local metabolic heat production., Indoor Air. 27 (2017) 261–272. doi:10.1111/ina.12324.

[12] G. Havenith, D. Fiala, Thermal Indices and Thermophysiological Modeling for Heat

Stress., Compr. Physiol. 6 (2015) 255–302. doi:10.1002/cphy.c140051.

[13] G. Havenith, R. Heus, W.A. Lotens, Resultant clothing insulation: a function of body movement, posture, wind, clothing fit and ensemble thickness., Ergonomics. 33 (1990) 67–84. doi:10.1080/00140139008927094.

[14] G. Havenith, R. Heus, W.A. Lotens, Clothing ventilation, vapour resistance and permeability index: Changes due to posture, movement and wind, Ergonomics. 33 (1990) 989–1005. doi:10.1080/00140139008925308.

[15] Y.S. Wu, J.T. Fan, W. Yu, Effect of posture positions on the evaporative resistance and thermal insulation of clothing, Ergonomics. 54 (2011) 301–313. doi:10.1080/00140139.2010.547604.

[16] E. Mert, A. Psikuta, M.A. Bueno, R.M. Rossi, The effect of body postures on the distribution of air gap thickness and contact area, Int. J. Biometeorol. (2016) 1–13. doi:10.1007/s00484-016-1217-9.

[17] E. Mert, A. Psikuta, M.A. Bueno, R.M. Rossi, Effect of heterogenous and homogenous air gaps on dry heat loss through the garment, Int. J. Biometeorol. 59 (2015) 1701–1710. doi:10.1007/s00484-015-0978-x.

[18] International Organization for Standardization, ISO 9920 Ergonomics of the thermal environment - Estimation of thermal insulation and water vapour resistance of a clothing ensemble, (2007) 104.

[19] J.S. Curlee, An approach for determining localized thermal clothing insulation for use in an element based thermoregulation and human comfort code, Master Thesis, Michigan Technological University, 2004.

[20] G. Havenith, D. Fiala, K. Blazejczyk, M. Richards, P. Bröde, I. Holmér, H. Rintamaki, Y. Benshabat, G. Jendritzky, The UTCI-clothing model, Int. J. Biometeorol. 56 (2012) 461–470. doi:10.1007/s00484-011-0451-4.

[21] S. Veselá, A. Psikuta, A.J.H. Frijns, Local clothing thermal properties of typical office ensembles under realistic static and dynamic conditions, Int. J. Biometeorol. (2018) 15. doi:10.1007/s00484-018-1625-0.

[22] Y. Lu, F. Wang, X. Wan, G. Song, C. Zhang, W. Shi, Clothing resultant thermal insulation determined on a movable thermal manikin. Part II: effects of wind and body movement on local insulation, 59 (2015) 1487–1498. doi:10.1007/s00484-015-0959-0.

[23] P.A. Nelson, D.A.;Curlee, J.S.;Curran, A.R.;Ziriax, J.M.; Mason, Determining localized garment insulation values from manikin studies: computational method and results, Eur J Appl Physiol. 95 (2005) 464–473. doi:10.1007/s00421-005-0033-4.

[24] E. McCullough, B. Jones, A comprehensive data base for estimating clothing insulation., ASHRAE Res. Proj. Reoprt RP-411. (1985) 162.

[25] J. Pokorný, J. Fišer, M. Fojtlín, B. Kopečková, R. Toma, J. Slabotínský, M. Jícha, Verification of Fiala-based human thermophysiological model and its application to protective clothing under high metabolic rates, Build. Environ. (2017).

doi:10.1016/j.buildenv.2017.08.017.

[26] E. Mert, S. Böhnisch, A. Psikuta, M.-A. Bueno, R.M. Rossi, Contribution of garment fit and style to thermal comfort at the lower body, Int. J. Biometeorol. 60 (2016) 1995–2004. doi:10.1007/s00484-016-1258-0.

[27] A. Psikuta, E. Mert, S. Annaheim, R.M. Rossi, Local air gap thickness and contact area models for realistic simulation of human thermo-physiological response, Int. J. Biometeorol. (2018) 1–14. doi:https://doi.org/10.1007/s00484-018-1515-5.

[28] E. Mert, A. Psikuta, M. Bueno, R.M. Rossi, The effect of body postures on the distribution of air gap thickness and contact area, Int. J. Biometeorol. 61 (2017) 363–375. doi:10.1007/s00484-016-1217-9.

[29] E. Mert, S. Böhnisch, A. Psikuta, M.-A. Bueno, R.M. Rossi, Contribution of garment fit and style to thermal comfort at the lower body, Int. J. Biometeorol. 60 (2016) 1995–2004. doi:10.1007/s00484-016-1258-0.

[30] A. Joshi, A. Psikuta, M.-A. Bueno, S. Annaheim, R.M. Rossi, Analytical clothing model for sensible heat transfer in skin-clothing-environment system considering spatial heterogeneity and natural convection, Int. J. Therm. Sci. Submitted manuscript (2018).

[31] International Organization for Standardization, EN ISO 14505-2 Ergonomics of the thermal environment - Evaluation of thermal environments in vehicles - Part 2: Determination of equivalent temperature, (2006) 25.

[32] International Organization for Standardization, ISO 15831 Clothing - Physiological effects - Measurement of thermal insulation by means of a thermal manikin, (2004) 11.

[33] K. Katic, R. Li, W. Zeiler, Thermophysiological models and their applications: A review, Build. Environ. 106 (2016) 286–300. doi:10.1016/j.buildenv.2016.06.031.

[34] H. Zhang, E. Arens, C. Huizenga, T. Han, Thermal sensation and comfort models for non-uniform and transient environments: Part I: Local sensation of individual body parts, Build. Environ. 45 (2010) 380–388. doi:10.1016/j.buildenv.2009.06.018.

[35] H. Zhang, E. Arens, C. Huizenga, T. Han, Thermal sensation and comfort models for non-uniform and transient environments, part II: Local comfort of individual body parts, Build. Environ. 45 (2010) 389–398. doi:10.1016/j.buildenv.2009.06.015.

[36] Q. Jin, X. Li, L. Duanmu, H. Shu, Y. Sun, Q. Ding, Predictive model of local and overall thermal sensations for non-uniform environments, Build. Environ. 51 (2012) 330–344. doi:10.1016/j.buildenv.2011.12.005.

[37] H.O. Nilsson, I. Holmér, Comfort climate evaluation with thermal manikin methods and computer simulation models., Indoor Air. 13 (2003) 28–37. doi:10.1034/j.1600-0668.2003.01113.x.

[38] Thermetrics, Seat Test Automotive Manikin, Prod. Broch. (2015) 2. http://www.thermetrics.com/sites/default/files/product_brochures/STAN Manikin Thermetrics 2015.pdf (accessed March 2, 2018).

[39] V.T. Bartels, Thermal comfort of aeroplane seats: Influence of different seat materials and the use of laboratory test methods, Appl. Ergon. 34 (2003) 393–399. doi:10.1016/S0003-6870(03)00058-9.

[40] M. Fojtlín, A. Psikuta, R. Toma, J. Fiser, M. Jícha, Determination of car seat contact area for personalised thermal sensation modelling, PLoS One. In press (2018).

[41] E.A.. McCullough, B.W.. Olsen, S.. Hong, Thermal insulation provided by chairs, ASHRAE Trans. Soc. Heat. Refrig. Airconditioning Engin. 100 (1994) 795–804. http://www.cbe.berkeley.edu/research/other-papers/McCullough et al 1994 Thermal insulation provided by chairs.pdf.

[42] T. Wu, W. Cui, B. Cao, Y. Zhu, Q. Ouyang, Measurements of the additional thermal insulation of aircraft seat with clothing ensembles of different seasons, Build. Environ. 108 (2016) 23–29. doi:10.1016/j.buildenv.2016.08.008.

[43] E. Mert, A. Psikuta, M.-A. Bueno, R.M. Rossi, Effect of heterogenous and homogenous air gaps on dry heat loss through the garment, Int. J. Biometeorol. 59 (2015) 1701–1710. doi:10.1007/s00484-015-0978-x.

[44] ASTM, F2370-16 Standard Test Method for Measuring the Thermal Insulation of Clothing Using a Heated Manikin, (2015) 1–7. doi:10.1520/F1291-15.1.

[45] A. Psikuta, Local air gap thickness and contact area models for realistic simulation of thermal effects in clothing, Int. J. Biometeorol. (2018) 1–14. doi:https://doi.org/10.1007/s00484-018-1515-5.

[46] D. Fiala, G. Havenith, Modelling Human Heat Transfer and Temperature Regulation, in: Mechanobiol. Mechanophysiology Mil. Inj., Springer, Berlin, 2015: pp. 265–302. doi:10.1007/978-3-319-33012-9.

[47] D. Fiala, K.J. Lomas, M. Stohrer, Computer prediction of human thermoregulatory and temperature responses to a wide range of environmental conditions, Int. J. Biometeorol. 45 (2001) 143–159. doi:10.1007/s004840100099.

[48] A. Psikuta, D. Fiala, G. Laschewski, G. Jendritzky, M. Richards, K. Blazejczyk, I. Mekjavič, H. Rintamäki, R. de Dear, G. Havenith, Validation of the Fiala multi-node thermophysiological model for UTCI application, Int. J. Biometeorol. 56 (2011) 443–460. doi:10.1007/s00484-011-0450-5.

[49] N. Martínez, A. Psikuta, K. Kuklane, J.I.P. Quesada, R.M.C.O. de Anda, P.P. Soriano, R.S. Palmer, J.M. Corberán, R.M. Rossi, S. Annaheim, Validation of the thermophysiological model by Fiala for prediction of local skin temperatures, Int. J. Biometeorol. 60 (2016) 1969–1982. doi:10.1007/s00484-016-1184-1.

[50] H.A.M. Daanen, A. Psikuta, 3D body scanning, in: Autom. Garment Manuf., 1st ed., Woodhead Publishing, 2017: pp. 237–252. doi:10.1016/B978-0-08-101211-6.00010-0.

[51] M. Fojtlín, J. Fišer, M. Jícha, Determination of convective and radiative heat transfer coefficients using 34-zones thermal manikin: Uncertainty and reproducibility evaluation, Exp. Therm. Fluid Sci. 77 (2016) 257–264. doi:10.1016/j.expthermflusci.2016.04.015.

[52] M.G.M. Richards, R. Rossi, H. Meinander, P. Broede, V. Candas, E. den Hartog, I. Holmér, W. Nocker, G. Havenith, Dry and Wet Heat Transfer Through Clothing Dependent on the Clothing Properties Under Cold Conditions, Int. J. Occup. Saf. Ergon. 14 (2015) 69–76. doi:10.1080/10803548.2008.11076750.

[53] F. Wang, C. Gao, K. Kuklane, I. Holmer, Determination of Clothing Evaporative Resistance on a Sweating Thermal Manikin in an Isothermal Condition : Heat Loss Method or Mass Loss Method?, Ann. Occup. Hyg. 55 (2011) 775–783. doi:10.1093/annhyg/mer034.

[54] B. Koelblen, A. Psikuta, A. Bogdan, S. Annaheim, R.M. Rossi, Comparison of fabric skins for the simulation of sweating on thermal manikins, Int. J. Biometeorol. 61 (2017) 1519–1529. doi:10.1007/s00484-017-1331-3.

[55] A. Mark, The impact of the individual layers in multi-layer clothing systems on the distribution of the air gap thickness and contact area, Master Thesis, Albstadt-Sigmaringen University of Applied Science, 2013.

[56] International Organization for Standardization, ISO 7730 Ergonomics of the thermal environment — Analytical determination and interpretation of thermal comfort using calculation of the PMV and PPD indices and local thermal comfort criteria, 3 (2005) 52.

[57] B.E. Ainsworth, W.L. Haskell, M.C. Whitt, M.L. Irwin, A.M. Swart, S.J. Strath, O.W. L, Compendium of Physical Activities: an update of activity codes and MET intensities, Med. Sci. Sport. Exerc. 32 (2000) 498–516.

[58] B. Koelblen, A. Psikuta, A. Bogdan, S. Annaheim, R.M. Rossi, Thermal sensation models: Validation and sensitivity towards thermo-physiological parameters, Build. Environ. 130 (2018) 200–211. doi:10.1016/j.buildenv.2017.12.020.

[59] T. Fukazawa, G. Havenith, Differences in comfort perception in relation to local and whole body skin wettedness, Eur. J. Appl. Physiol. 106 (2009) 15–24. doi:10.1007/s00421-009-0983-z.

[60] H.A.M. Daanen, E. Van De Vliert, X. Huang, Driving performance in cold, warm, and thermoneutral environments, Appl. Ergon. 34 (2003) 597–602. doi:10.1016/S0003-6870(03)00055-3.

[61] A. Psikuta, J. Frackiewicz-Kaczmarek, E. Mert, M.A. Bueno, R.M. Rossi, Validation of a novel 3D scanning method for determination of the air gap in clothing, Meas. J. Int. Meas. Confed. 67 (2015) 61–70. doi:10.1016/j.measurement.2015.02.024.

[62] G. Havenith, M.G. Richards, X. Wang, P. Brode, V. Candas, E. den Hartog, I. Holmer, K. Kuklane, H. Meinander, W. Nocker, Apparent latent heat of evaporation from clothing: attenuation and "heat pipe" effects, J. Appl. Physiol. 104 (2007) 142–149. doi:10.1152/japplphysiol.00612.2007.

[63] S. Ueno, S.I. Sawada, Correction of the evaporative resistance of clothing by the temperature of skin fabric on a sweating and walking thermal manikin, Text. Res. J. 82 (2012) 1143–1156. doi:10.1177/0040517511427966.

[64] F. Wang, K. Kuklane, C. Gao, I. Holmér, Development and validity of a universal

empirical equation to predict skin surface temperature on thermal manikins, J. Therm. Biol. 35 (2010) 197–203. doi:10.1016/j.jtherbio.2010.03.004.